AFDELINGEN FOR
BÆRENDE KONSTRUKTIONER
DANMARKS TEKNISKE HØJSKOLE

STRUCTURAL RESEARCH LABORATORY
TECHNICAL UNIVERSITY OF DENMARK

M. W. Bræstrup, M. P. Nielsen, B. Chr. Jensen
and Finn Bach

AXISYMMETRIC PUNCHING OF PLAIN AND REINFORCED CONCRETE

RAPPORT NR. R 75 1976

AXISYMMETRIC PUNCHING OF PLAIN AND REINFORCED CONCRETE

by

M.W.Bræstrup, lic.techn.
M.P.Nielsen, dr.techn.
B.Chr.Jensen, lic.techn.
Finn Bach, lic.techn.

Structural Research Laboratory
Technical University of Denmark

ABSTRACT

An upper-bound solution is found, assuming the concrete to be rigid, perfectly plastic with the modified Coulomb failure criterion as yield condition and the associated flow rule. The shape of the failure surface is determined by variational calculus. The generatrix is a catenary curve, possibly in combination with a straight line. The optimum diameter of the intersection with the bottom face of the slab and the corresponding ultimate load are plotted as functions of slab depth, punch diameter, and the tensile and compressive concrete strengths. The solution is compared with test results and good qualitative agreement and fair quantitative agreement are found.

TABLE OF CONTENTS

INTRODUCTION

The design of reinforced concrete slabs against punching shear is based upon rules laid down in the building codes. These rules contain empirical formulae derived from experience and bear little or no relation to a rational analysis of the problem using available theories of applied mechanics. In the present paper, shear punching failure is treated by the upper-bound technique of the theory of plasticity. The results do not only apply to punching of slabs, but also to the load-carrying capacity of inserts imbedded in concrete. In particular, the analysis constitutes a theoretical justification for the application of pull-out tests to determine the compressive strength of concrete.

The basic assumptions are specified in the section below. They consist in:

(a) An assumption about concrete as a perfectly plastic material.

(b) An assumption about the failure mechanism.

Assumption (b) is an idealization of a behaviour which is amply supported by experience, whereas assumption (a) amounts to a drastically simplified description of concrete. The deformability of the material is very limited, especially in tension, and the validity of the normality condition is open to serious doubt. On the other hand, the analysis of shear in beams [1],[2] and joints [3] has shown that useful results can indeed be obtained using the theory of plasticity for concrete. It must be stressed, however, that results of this kind should not be used without thorough experimental checking. With this in mind, the theory serves as a rational explanation of the phenomena observed in reality.

NOTATIONS

Symbols are defined when they first occur in the text. The repeatedly used notations are listed below:

a, b, c	:	Constants of catenary curve (equation(5))
D	:	Diameter of support (counterpressure)
d	:	Diameter of punch (Figure 4)
d_1	:	Diameter of intersection of failure surface with bottom face of slab (Figure 4)
F	:	Function of r and r' (equation(2b))
f_c	:	Compressive concrete (cylinder) strength
f_t	:	Tensile concrete strength
h	:	Slab (imbedment) depth (Figure 4)
h_o	:	Depth of conical failure surface (Figure 5)
k	:	Material constant (Figure 2). $k = (1+\sin\varphi)/(1-\sin\varphi)$
P	:	Ultimate punching load
p	:	Distributed counterpressure
r	:	Distance of failure surface from centreline (Figure 4)
r'	:	Derivative of r with respect to x
s_y	:	Yield force of shear reinforcement per unit area perpendicular to reinforcing bars
W_E	:	Rate of external work
W_I	:	Rate of internal work
w_I	:	Rate of internal work per unit area of failure surface
x	:	Coordinate (distance) along slab normal (Figure 4)

α : Angle between rate of deformation and failure surface (Figure 4)

α_o : Half angle of conical failure surface

γ : Angle between shear reinforcement and slab (Figure 10)

δ : Rate of deformation (Figure 4)

ε_1, ε_2 : Principal strain rates (Figure 2)

λ : Material constant. $\lambda = 1 - \rho(k-1)$

μ : Material constant. $\mu = 1 - \rho(k+1)$

ν : Effectiveness factor. $\nu = f_c^*/f_c$

ρ : Relative tensile strength. $\rho = f_t/f_c$

σ_1, σ_2 : Principal stresses (Figure 2)

τ : Shear stress. $\tau = P/\pi(d+h)h$

φ : Angle of friction

χ : Relative distributed load. $\chi = p/f_c$

ψ : Degree of shear reinforcement. $\psi = s_y/f_c$

BASIC ASSUMPTIONS

Figure 1 shows a concrete slab annularly supported and centrally loaded by a circular punch. The slab is reinforced in such a way that flexural failure is prevented. The analysis of punching shear failure presented below is based upon the assumptions:

(a) The concrete is rigid, perfectly plastic with the modified Coulomb failure criterion as yield condition. The angle of friction is φ, the uniaxial compressive and tensile strength being f_c and $f_t = \rho f_c$, respectively. The deformations are governed by the associated flow rule (normality condition).

(b) The failure mechanism consists in the punching out of a solid of revolution, the rest of the slab remaining rigid (cf. Figure 1). The failure surface is in a plane state of strain.

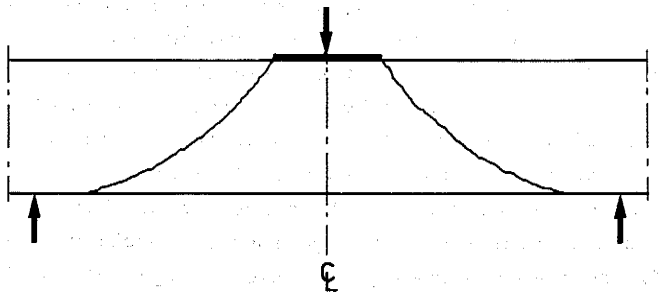

Figure 1: Punching shear failure

The modified Coulomb failure criterion consists of a condition of sliding failure:

$$\tau = c - \sigma\tan\varphi$$

and a condition of separation failure:

$$\sigma = \rho f_c$$

Here τ and σ are shear and normal stress, respectively, on an arbitrary section in the material. The cohesion c is related to the compressive strength f_c by the expression:

$$f_c = 2c\sqrt{k} \quad ,$$

where the constant k is determined by the angle of friction:

$$k = \frac{1 + \sin\varphi}{1 - \sin\varphi}$$

The yield locus in the case of plane strain is shown on Figure 2. The principal stresses are σ_1 and σ_2, and the corresponding principal strain rates are termed ε_1 and ε_2. The normality condition requires the vector $(\varepsilon_1, \varepsilon_2)$ to be an outward directed normal to the yield locus. Hence we deduce that:

Stress regime AB :		σ_1 =	ρf_c
	$(k\rho-1)f_c$ <	σ_2 <	ρf_c
corresponds to		$\varepsilon_2/\varepsilon_1$ =	0
Stress regime B :		σ_1 =	ρf_c
		σ_2 =	$(k\rho-1)f_c$
corresponds to	- 1/k <	$\varepsilon_2/\varepsilon_1$ <	0
Stress regime BC :		σ_1 <	ρf_c
		σ_2 =	$k\sigma_1 - f_c$
corresponds to		$\varepsilon_2/\varepsilon_1$ =	-1/k

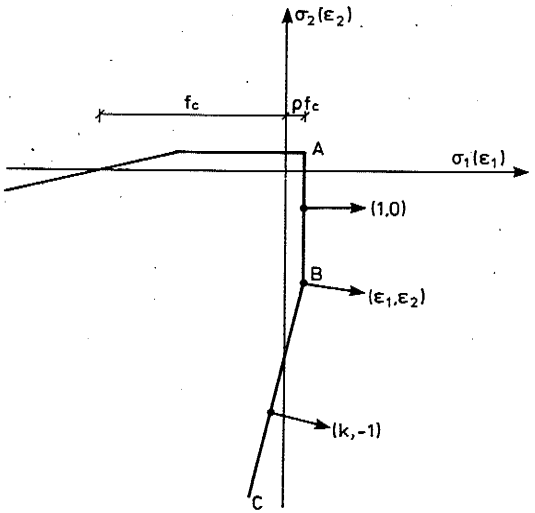

Figure 2: Yield locus and flow rule for plane strain

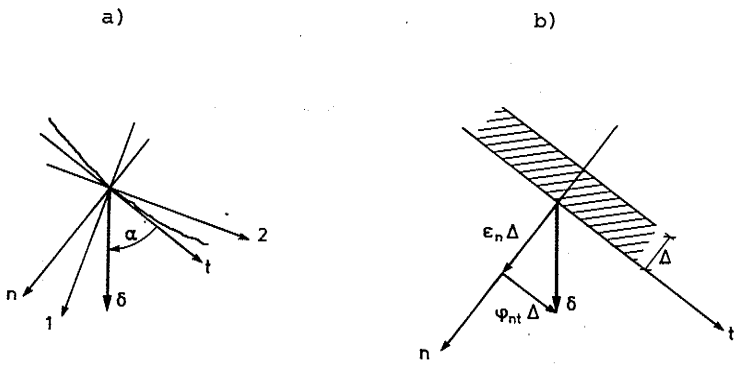

Figure 3: Normal section of failure surface
a: Kinematical discontinuity
b: Narrow region with homogeneous strain rates

Note that the normality condition excludes the situation $\varepsilon_2/\varepsilon_1 < -1/k$.

Consider a kinematical discontinuity (failure surface). The relative velocity is δ , directed at the angle α to the discontinuity. Figure 3a shows the intersection of the failure surface with the plane determined by the surface normal n and the velocity vector δ . The discontinuity is an idealization of a narrow region of depth Δ with a high, homogeneous strain rate δ/Δ (cf. Figure 3b).

The local components of the homogeneous strain rate are:

$$\varepsilon_n = \frac{\delta}{\Delta} \sin\alpha$$

$$\varepsilon_t = 0$$

$$\varphi_{nt} = 2\gamma_{nt} = \frac{\delta}{\Delta} \cos\alpha$$

The principal strain rates are given by:

$$\left.\begin{matrix}\varepsilon_1 \\ \varepsilon_2\end{matrix}\right\} = \frac{1}{2}(\varepsilon_n+\varepsilon_t) \pm \sqrt{\frac{1}{4}(\varepsilon_n-\varepsilon_t)^2+\gamma_{nt}^2} = \begin{cases} \frac{1}{2}\delta(1+\sin\alpha)/\Delta \\ -\frac{1}{2}\delta(1-\sin\alpha)/\Delta \end{cases}$$

The principal directions are as indicated on Figure 3a. The first principal axis bisects the angle between the rate of deformation and the surface normal.

The rate of internal work dissipated per unit area of the failure surface is:

$$w_I = (\varepsilon_1\sigma_1 + \varepsilon_2\sigma_2)\Delta ,$$

where the principal stresses are determined by the flow rule. Since $\varepsilon_1/\varepsilon_2 = -k$ for $\alpha = \varphi$, the rate of internal work w_I as a function of the angle α is given as follows:

$\alpha = \pi/2$ (Stress regime AB)

$$w_I = \delta\rho f_c$$

$\varphi < \alpha < \pi/2$ (Stress regime B)

$$w_I = \frac{1}{2}\delta(1+\sin\alpha)\rho f_c - \frac{1}{2}\delta(1-\sin\alpha)(k\rho-1)f_c$$

$$w_I = \frac{1}{2}\delta f_c[(\rho-k\rho+1)+(\rho+k\rho-1)\sin\alpha]$$

$$w_I = \frac{1}{2}\delta f_c(\lambda-\mu\sin\alpha) \qquad (1)$$

$\alpha = \varphi$ (stress regime BC)

$$w_I = \frac{1}{2}\delta(1+\sin\varphi)\sigma_1 - \frac{1}{2}\delta(1-\sin\varphi)(k\sigma_1-f_c)$$

$$w_I = \frac{1}{2}\delta f_c(1-\sin\varphi)$$

$\alpha < \varphi$ is not allowable.

The parameters λ and μ are defined as

$$\lambda = 1 - \rho(k-1)$$

$$\mu = 1 - \rho(k+1)$$

Note that equation (1) is valid in the closed interval $\varphi \leq \alpha \leq \pi/2$, and that at the end points the rate of internal work depends exclusively upon the compressive, respectively the tensile strength.

UPPER BOUND SOLUTION

An upper bound P for the ultimate punching load is found by equating the rate of work done by the load to the rate of work dissipated in the failure surface. The rate of external work is:

$$W_E = P\delta$$

The rate of internal work is found by integration over the failure surface:

$$W_I = \int w_I \, dA \quad ,$$

where w_I is given by equation (1). The failure surface is sketched on Figure 4. Punch diameter and slab depth are termed d and h, respectively, and the generatrix of the surface is described by the function $r = r(x)$, the coordinate axes being shown on the figure. The area element can then be taken as

$$dA = 2\pi r \frac{dx}{\cos\alpha}$$

The work equation yields:

$$W_E = W_I$$

$$P\delta = \int_o^h \frac{1}{2}\delta f_c(\lambda - \mu\sin\alpha)\, 2\pi r \frac{dx}{\cos\alpha}$$

Introduction of the relation $\tan\alpha = \frac{dr}{dx} = r'$, leads to the upper bound:

$$P = \pi f_c \int_o^h F(r,r')dx \qquad (2a)$$

where

$$F(r,r') = r(\lambda\sqrt{1+(r')^2} - \mu r') \qquad (2b)$$

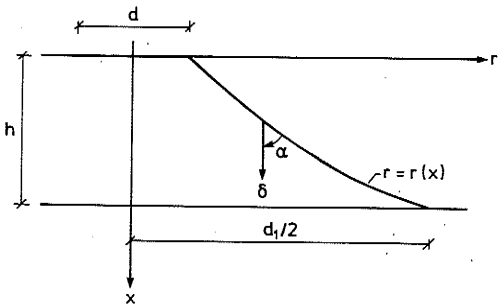

Figure 4: Failure surface generatrix

Assume a failure surface in the shape of a truncated cone with half angle α_o . Then

$$r = \frac{d}{2} + x\tan\alpha_o$$

$$r' = \tan\alpha_o$$

$$F(r,r') = \left(\frac{d}{2} + x\tan\alpha_o\right) \frac{\lambda - \mu\sin\alpha_o}{\cos\alpha_o}$$

and the upper bound becomes

$$P = \pi f_c \int_o^h F(r,r')dx$$

$$P = \pi f_c \frac{h}{2} \frac{(d\cos\alpha_o + h\sin\alpha_o)(\lambda - \mu\sin\alpha_o)}{\cos^2\alpha_o} \qquad (3)$$

The shape of the failure surface which corresponds to the lowest upper bound is determined by calculus of variations. The problem amounts to finding the function $r(x)$ that minimizes the integral $\int_o^h F(r,r')dx$. The Euler equation is (cf. [4], p.206):

$$F - r'F_{r'} = c_1 \quad ,$$

c_1 being a constant. The function F is given by equation (2b), hence:

$$r(\lambda\sqrt{1+(r')^2} - \mu r') - r'r(\lambda \frac{r'}{\sqrt{1+(r')^2}} - \mu) = c_1$$

This may be reduced to:

$$1 + (r')^2 = r^2/c^2 \tag{4a}$$

or

$$r'' = r/c^2 \tag{4b}$$

where

$$c = c_1/\lambda$$

The complete solution to equation (4b) is:

$$r = a\cosh \frac{x}{c} + b\sinh \frac{x}{c} \tag{5}$$

This function satisfies equation (4a) provided that $c^2=a^2-b^2$, and without loss of generality we may take

$$c = \sqrt{a^2-b^2}$$

The constants a and b are determined by the boundary conditions. $r = d/2$ for $x = 0$, yields $a = d/2$. If $2r = d_1$ for $x = h$, then b is found from the equation:

$$\frac{d_1}{2} = a\cosh \frac{h}{c} + b\sinh \frac{h}{c}$$

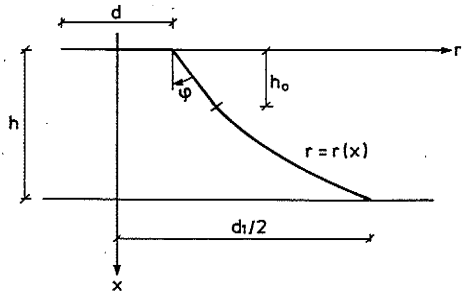

Figure 5: Optimal failure surface generatrix

The angle α between the velocity δ and the failure surface is given by:

$$\tan\alpha = r' = \frac{a}{c}\sinh\frac{x}{c} + \frac{b}{c}\cosh\frac{x}{c}$$

The minimum value $\tan\alpha = b/c$ is obtained at $x = 0$. Assumption (a) of the preceding section requires that $b/c \geq \tan\varphi$. For some values of d, h, and d_1, this condition cannot be satisfied by the function given by equation (5). In such cases, the failure surface generatrix will consist of a straight line in combination with the catenary curve, as sketched on Figure 5. The generatrix $r = r(x)$ is then:

$$r = \frac{d}{2} + x\tan\varphi \qquad \text{for } 0 \leq x \leq h_o \qquad (6a)$$

$$r = a\cosh\frac{x-h_o}{c} + b\sinh\frac{x-h_o}{c} \qquad \text{for } h_c \leq x \leq h \qquad (6b)$$

The four constants h_o, a, b, and c are determined by the equations:

$$c = \sqrt{a^2-b^2} \tag{7a}$$

$$a = \frac{d}{2} + h_o \tan\varphi \qquad (x=h_o) \tag{7b}$$

$$\tan\varphi = \frac{b}{c} \qquad (x=h_o) \tag{7c}$$

$$\frac{d_1}{2} = a \cosh \frac{h-h_o}{c} + b \sinh \frac{h-h_o}{c} \qquad (x=h) \tag{7d}$$

The lowest upper bound for the ultimate load is found from equations (2), the function $r(x)$ being given by equations (6). Thus P is the sum of two parts:

$$P = P_1 + P_2 \tag{8a}$$

where P_1 and P_2 are the contributions from the conical surface and the catenary of revolution, respectively.

P_1 is found from equation (3) with $\alpha_o = \varphi$ and $h = h_o$:

$$P_1 = \pi f_c \frac{h_o}{2} \frac{(d\cos\varphi + h_o \sin\varphi)(1-\sin\varphi)}{\cos^2\varphi} \tag{8b}$$

Equations (2) yield:

$$P_2 = \pi f_c \int_{h_o}^{h} r(\lambda\sqrt{1+(r')^2} - \mu r')\,dx$$

Here $rdx = c^2 d(r')$ by equation (4b), hence

$$\begin{aligned}
\int F(r,r')dx &= \lambda \int \sqrt{1+(r')^2}\, c^2 d(r') - \mu \int r\, dr \\
&= \lambda c^2 [\frac{r'}{2}\sqrt{1+(r')^2} + \frac{1}{2}\ln(r'+\sqrt{1+(r')^2})] - \frac{1}{2}\mu r^2 + C_1 \\
&= \lambda c^2 \frac{r'}{2}\frac{r}{c} + \frac{1}{2}\lambda c^2 \ln(r'+\frac{r}{c}) - \frac{1}{2}\mu r^2 + C_1 \\
&= \frac{1}{2}\lambda c^2 \ln[\frac{a+b}{c}(\cosh\frac{x-h_o}{c} + \sinh\frac{x-h_o}{c})] + \frac{1}{2}r(\lambda cr' - \mu r) + C_1 \\
&= \frac{1}{2}\lambda c(x-h_o) + \frac{1}{2}r[\lambda(b\cosh\frac{x-h_o}{c} + a\sinh\frac{x-h_o}{c}) \\
&\qquad - \mu(a\cosh\frac{x-h_o}{c} + b\sinh\frac{x-h_o}{c})] + C
\end{aligned}$$

where equations (4a) and (6b) have been used, and

$$C = C_1 + \frac{1}{2}\lambda c^2 \ln \frac{a+b}{c}$$

Thus:

$$P_2 = \pi f_c[\frac{1}{2}\lambda c(h-h_o) + \frac{1}{2}\frac{d_1}{2}(\lambda(b\cosh\frac{h-h_o}{c} + a\sinh\frac{h-h_o}{c}) - \mu(a\cosh\frac{h-h_o}{c} + b\sinh\frac{h-h_o}{c})) - \frac{1}{2}a(\lambda b - \mu a)$$

Using equations (7a) and (7d), this may be reduced to (cf. KÆRN & JENSEN [5]):

$$P_2 = \frac{1}{2}\pi f_c[\lambda c(h-h_o) + \lambda(\frac{d_1}{2}\sqrt{(\frac{d_1}{2})^2 - c^2} - ab) - \mu((\frac{d_1}{2})^2 - a^2)] \quad (8c)$$

ANALYTICAL RESULTS

The values of $\tan\varphi$, f_c , and ρ , as well as the punch diameter d , support diameter D , and slab thickness h are assumed to be given. The shape of the optimal failure surface and the corresponding least upper bound are found by iteration on an electronical computer. The strategy of the iteration process is as follows:

(1) Assume a value of the opening diameter d_1, i.e. the diameter of the intersection of the failure surface with the bottom of the slab.

(2) Assume $h_o = 0$

(3) Determine the constant a from equation (7b) and assume a value of the constant b .

(4) Calculate c by equation (7a) and the radius r_1 given by the right hand side of equation (7d). If r_1 is not sufficiently close to $d_1/2$, change the value of b and repeat the step.

(5) If $h = 0$, check if $b/c \geq \tan\varphi$. If this is not the case, assume a value $h_o \neq 0$ and repeat the process from (3).
If $h \neq 0$, check if equation (7c) is satisfied.
If not, change the value of h_o and repeat the process from (3).

(6) Determine P by equations (8)

By this procedure a failure surface and an upper bound P is obtained corresponding to the choice of d_1 . The value of d_1 which gives the least upper bound is very dependent upon the assumed tensile concrete strength, i.e. upon the value of ρ . For $\rho = 0$, P decreases with increasing d_1 , which means

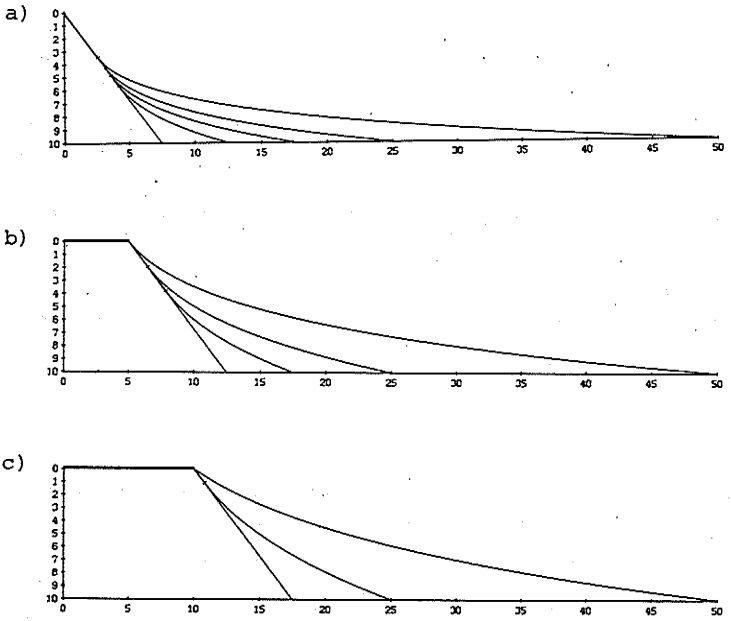

Figure 6: Failure surface generatrices corresponding to zero concrete strength

a) d/h = 0. D/h = 1.5, 2.5, 3.5, 5, and 10

b) d/h = 1. D/h = 2.5, 3.5, 5, and 10

c) d/h = 2. D/h = 3.5, 5, and 10

Figure 7: Punching load for zero tensile concrete strength

a) Load parameter as function of relative support diameter for various values of relative punch diameter.

b) Load parameter as function of relative punch diameter for various values of relative support diameter.

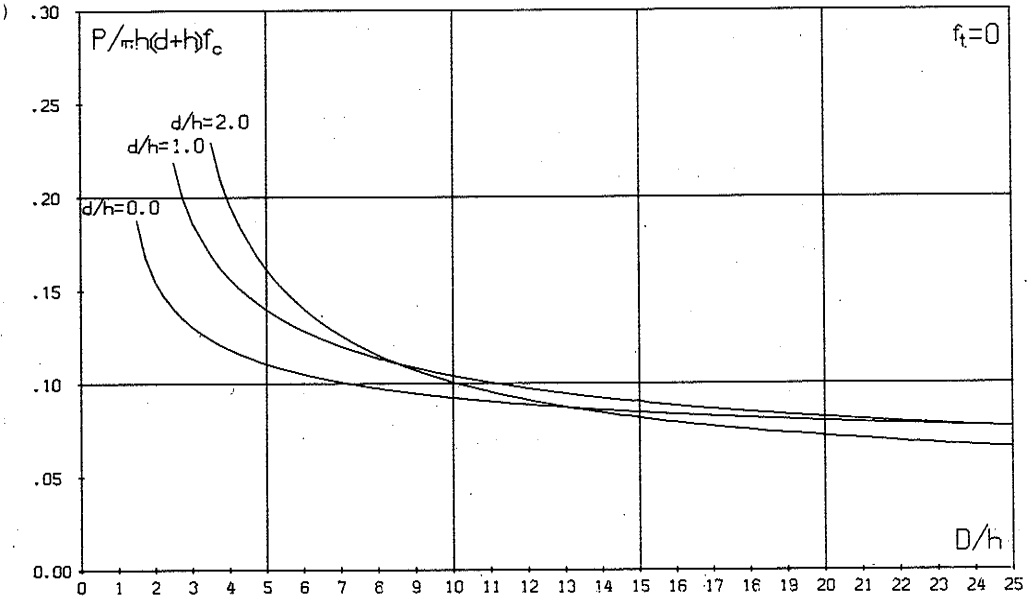
P/πh(d+h)f_c
f_t=0
d/h=2.0
d/h=1.0
d/h=0.0
D/h
.30
.25
.20
.15
.10
.05
0.00
0 1 2 3 4 5 6 7 8 9 10 11 12 13 14 15 16 17 18 19 20 21 22 23 24 25

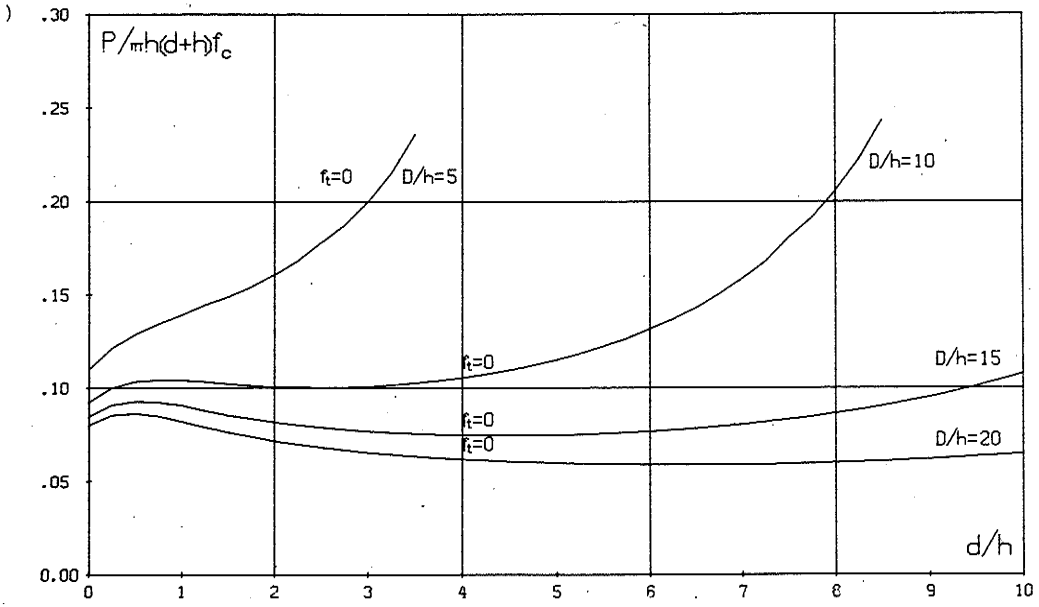
P/πh(d+h)f_c
f_t=0
D/h=5
D/h=10
f_t=0
D/h=15
f_t=0
f_t=0
D/h=20
d/h
.30
.25
.20
.15
.10
.05
0.00
0 1 2 3 4 5 6 7 8 9 10

that the failure surface will always extend all the way to the support, i.e. $d_1 = D$. Examples of failure surface generatrices are shown on Figure 6. The angle of friction is assumed to be φ with $\tan\varphi = 0.75$. This angle is used in all the calculations below. The shape of the surface is determined by the relative punch diameter d/h and the relative support diameter D/h.
As non-dimensional load parameter it turns out to be very convenient to use the quantity τ/f_c, where $\tau = P/\pi(d+h)h$ is the nominal shear stress on a cylindrical surface with diameter d+h. The load parameter is plotted as a function of the relative support diameter on Figure 7a. The result is rather insensitive to the value of φ assumed, except for the smallest support diameters. The load approaches zero asymptotically as

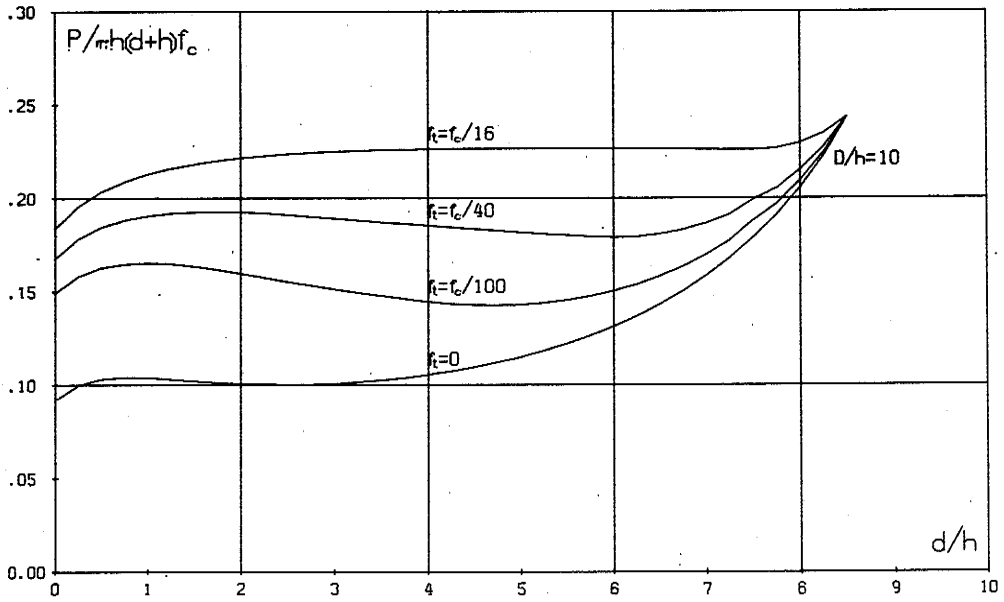

Figure 8: Punching load for various levels of tensile concrete strength

the support diameter increases towards infinity. Figure 7b shows the load parameter as a function of the relative punch diameter. Note (on both figures) that when the punch diameter is not too big compared with the support diameter, then the load parameter is fairly independent of the relative punch diameter. This fact corroborates the design method of the CEB building code [6], which is based upon the nominal shear stress τ defined above.

The introduction of a finite tensile strength (i.e. $\rho \neq 0$) leads to a finite value of the optimum opening diameter d_1. This value is found by iteration. As a starting point is chosen $d_1' = d + 2h\tan\varphi$. The support diameter must not be less than this value in order to comply with the condition $\alpha \geq \varphi$. The corresponding upper bound is found by the procedure described by points (2)-(6) above. The diameter d_1 is then increased until a minimum of P is found or $d_1 = D$. When the support diameter is greater than the optimum opening diameter, then the ultimate load becomes independent of the support diameter (cf. Figure 15 of the section that follows). The load parameter is still fairly independent of the relative punch diameter, as seen on Figure 8 (cf. also Figure 14 below).

From Figure 8, it appears that the tensile strength has a considerable influence upon the load-carrying capacity. It is worthy of note, however, that the ultimate load is independent of the tensile strength, provided the support diameter has the value $D = d + 2h\tan\varphi$. In this case, the failure surface degenerates into a truncated cone (cf. Figure 6) and the ultimate load is given by equation (3) with $\alpha_o = \varphi$, i.e.:

$$P = \pi f_c \, h(d + h\tan\varphi) \, \frac{1-\sin\varphi}{\cos\varphi} \qquad (9)$$

Thus P is proportional to f_c. This means that if the condition $D = d + 2h\tan\varphi$ is satisfied - at least approximately - by the experimental setup, then punching tests may be used to determine the compressive concrete strength (cf. JENSEN & BRÆSTRUP [7].

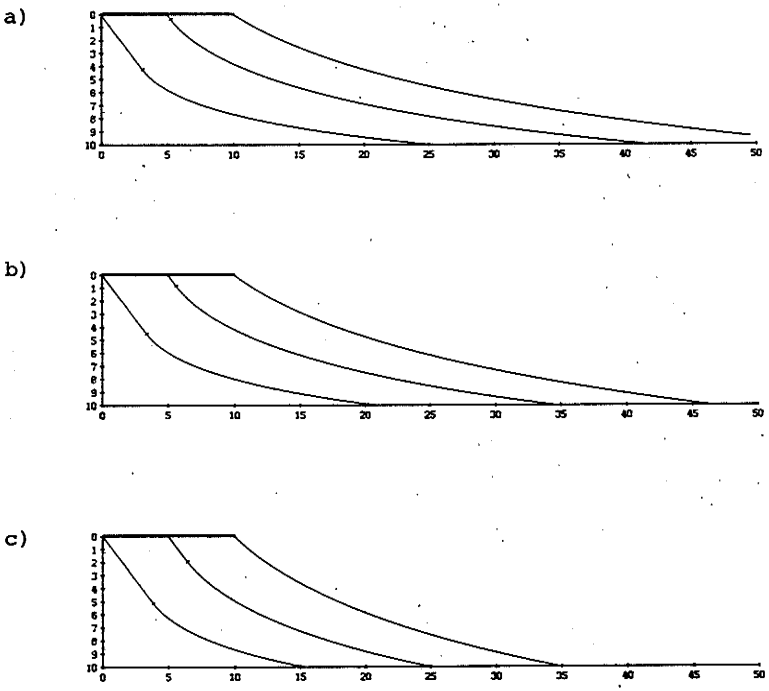

Figure 9: Optimum failure generatrices corresponding to various levels of tensile concrete strength.

a): ρ = 1/400. d/h = 0, 1, and 2

b): ρ = 1/250. d/h = 0, 1, and 2

c): ρ = 1/100. d/h = 0, 1, and 2

Figure 9 shows examples of optimum failure generatrices. The support diameter is supposed to be greath enough so as not to interfere with the solution. The optimal diameter is an approximately linear function of the punch diameter, as seen on Figure 12 of the section below.

The presence of a uniform counterpressure - as when a column is punching a slab carrying distributed load - has an effect very similar to that of the tensile strength. If the load

per unit area is $p = \chi f_c$, then the solution depends upon the factor χ in much the same way as on the factor ρ . This goes for the shape of the failure surface (cf. Figure 9) as well as for the ultimate load (cf. Figure 8).

The effect of a continuously distributed shear reinforcement is exactly the same as that of a distributed counterpressure. Let the shear reinforcement degree be $\psi = s_Y/f_c$, where s_Y is the yield force per unit area perpendicular to the reinforcing bars, and let the bars be inclined at the angle γ to the slab (cf. Figure 10). The reinforcement is assumed to be rigid, perfectly plastic and able to resist forces in the direction of the bars only. Then the quantity $\psi \sin^2\gamma$ will correspond to the factor χ , introduced above.

In practice, the shear reinforcement - if any - will be confined to a region around the punch (or column) and not distributed over the entire slab. In that case, the reinforcement will not affect the shape of the failure surface, but enhance the ultimate load by the contribution $S_Y \sin\gamma$, S_Y being the total yield force of the reinforcement. This is only correct, however, provided that a lower upper bound cannot be obtained with a failure surface completely inside or completely outside the shear reinforcement (see Figure 10).

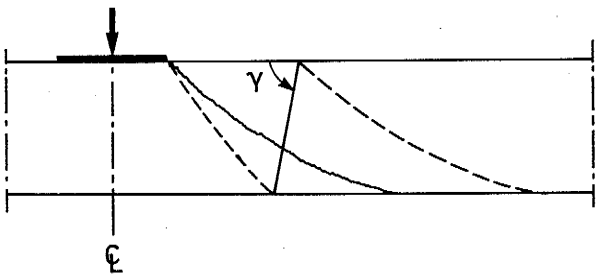

Figure 10: Punching of slab with shear reinforcement. With dotted lines are indicated possible failure surfaces not activating the reinforcement.

EXPERIMENTAL RESULTS

The shape of the failure surface may be investigated experimentally by studying the pieces of material punched out of test specimens. BACHE & ISEN [8] produced artificial pop-outs

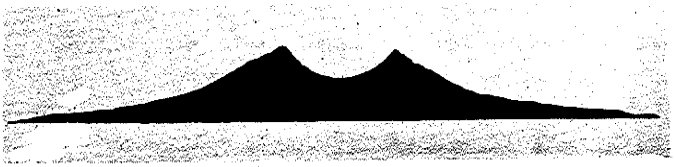

Figure 11: Profile of artificial pop-out, produced by hydraulic pressure inside a rubber ball imbedded in a mortar specimen (Reproduced from [8]).

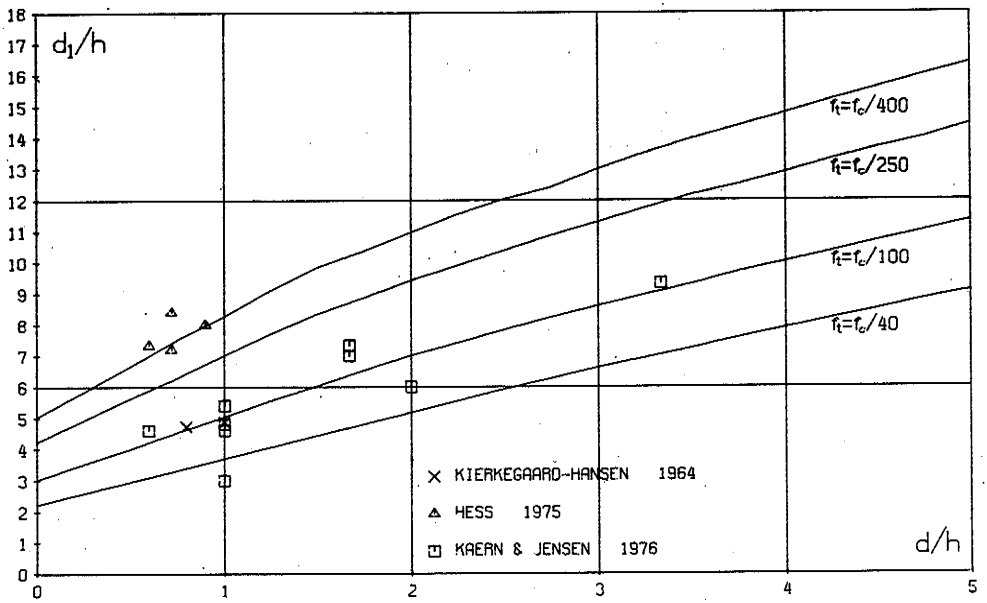

Figure 12: Relative failure surface opening diameter plotted against relative punch diameter

by inflating a rubber ball imbedded near the end face of a mortar cylinder. A failure profile is shown on Figure 11, and the shape agrees reasonably well with the theoretical predictions of the preceding section. Note the thinness of the pop-out near the edge.

Pull-out tests on plain concrete blocks were performed by HESS [9]. Two 36 mm diameter steel discs mounted on shafts were imbedded at the centres of opposite faces of the specimen, and a tensile force was applied to both shafts. Again, a striking feature of the failure is the shallowness of the crater. A total of 11 tests were carried out, but only in four cases (imbedment depth less then 80 mm) could the failure be contained within the 500×500 mm^2 face of the block. The opening diameters d_1 have been measured on the (unpublished) failure photographs and are plotted on Figure 12 together with the theoretical curves determined above.

Most tests reported in the literature are one-sided, which means that a counterpressure (support) is applied. An experimental investigation carried out by KIERKEGAARD-HANSEN [10] includes a test series with relative punch diameters close to 1 and the author reports that the failure was contained within the support diameter, which was 5-6 times the imbedment depth. One of the failures is seen on Figure 13. The disc was punched out by means of a mandrel pushed downwards through the specimen. The shape of two fracture pieces were measured, and the results are plotted on Figure 12.

The failure surfaces produced by punching of slabs are generally disturbed by the presence of bottom reinforcement. However, KÆRN & JENSEN [5] have carried out 12 tests using reinforcement in the circumferential direction only. Slab depths of 30 and 50 mm were used, and the punch diameter varied between 30 and 100 mm. All the failures took place within the 300 mm support diameter. The opening diameters were measured on the original failure photographs (reproduced in [5]) and the results are plotted on Figure 12.

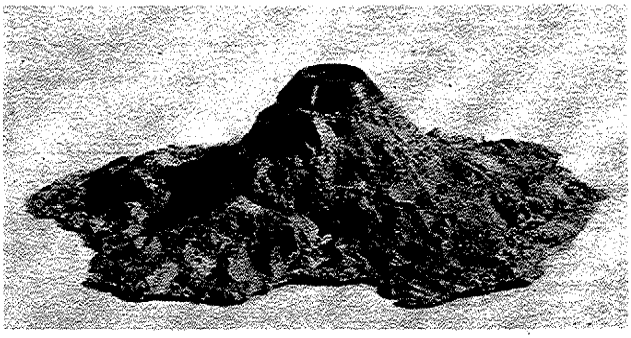

Figure 13: Piece of material punched out of concrete specimen. (Reproduced from [10])

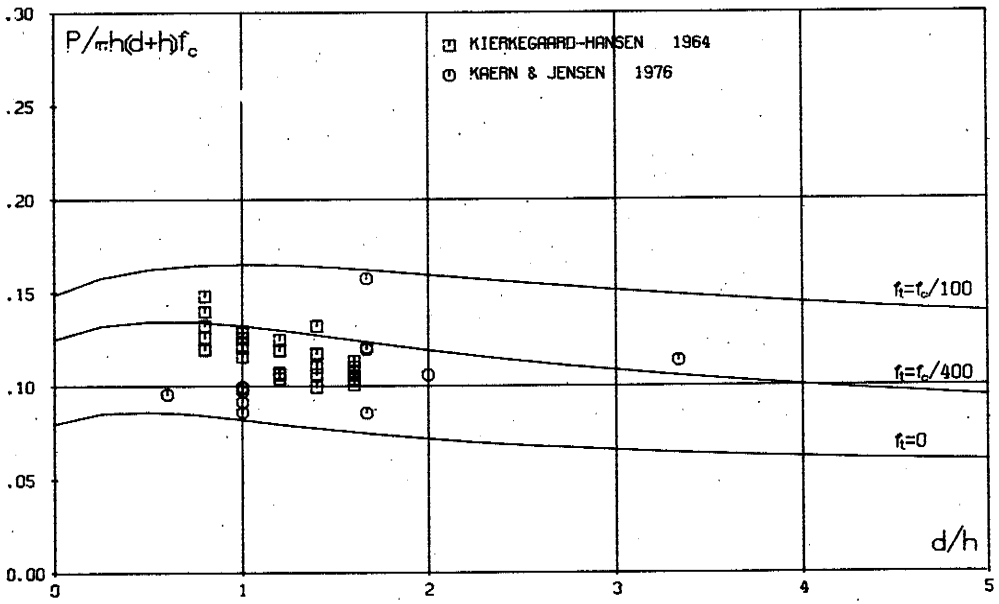

Figure 14: Load parameter plotted against relative punch diameter. Support diameter greater than optimum opening diameter.

The determination of the experimental opening diameter is a somewhat tricky business, due to the irregularity of the failure crater. KIERKEGAARD-HANSEN [10] measured the projected area of the failure surface (cf. Figure 13) and the value of d_1 plotted is the diameter of a circle with the same area. In the other cases, the diameters are judged from photographs taken after failure.

The diagram of Figure 12 shows a marked difference between the free failures from [9] and the failures with supports [5] and [10]. This suggests the conclusion that the presence of a counterpressure may have a disturbing effect upon the development of the failure, although the failure surface does not reach the support. Apart from that, the variation of the opening diameter with the punch diameter conforms rather well with the theoretical prediction.

The ultimate loads from KÆRN & JENSEN [5] and the series from KIERKEGAARD-HANSEN [10] mentioned above are plotted on Figure 14 against the punch diameter. The theoretical curves shown correspond to a support diameter which is too great to affect the solution. The points corresponding to [10] lie close together, whereas the results from [5] are more scattered. As predicted, there seems to be no systematic variation of the load parameter with the relative punch diameter.

Most of the tests described in reference [10] we carried out with $d = h = 25$ mm, and the investigation includes three series where only the support diameter was varied. The concrete cylinder strengths were 118, 294, and 395 kp/cm^2, respectively. The ultimate loads are plotted on Figure 15, with the exception of two tests where the loading was interrupted because of misalignment of the setup. The plot also includes the results from Figure 14 which had $d = h$. The tests from [10] had concrete strengths between 201 and 214 kp/cm^2, whereas the concrete strengths of KÆRN & JENSEN [5] varied between 16.9 and 30.7 N/mm^2.

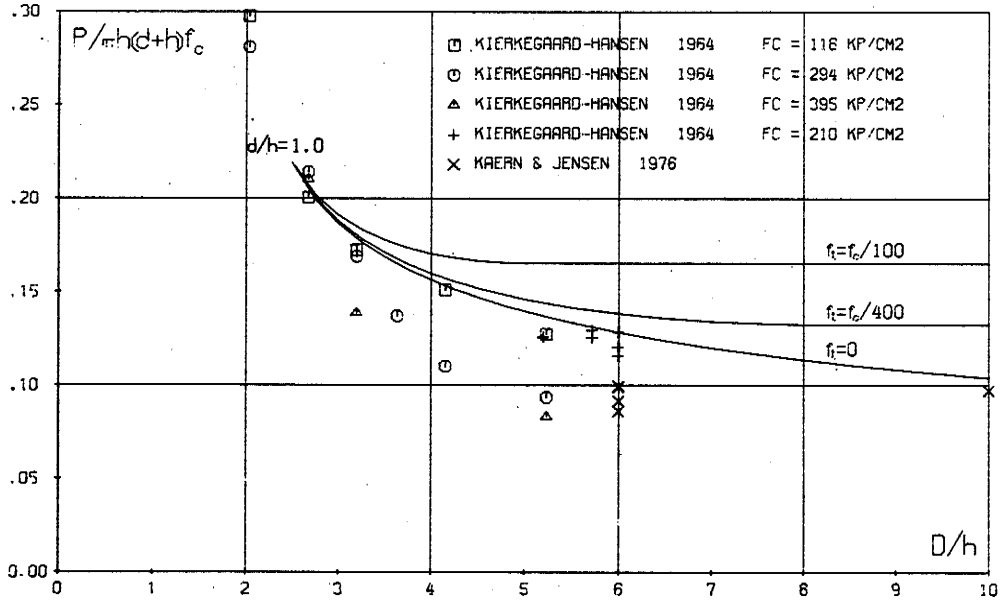

Figure 15: Load parameter plotted against relative support diameter. Punch diameter equal to slab (imbedment) depth.

Figure 15 shows the theoretical curves for d/h = 1 corresponding to various levels of relative tensile strength. One of the series is seen to fit extraordinarily well to the curve for $\rho = 0$, but the majority of the ultimate loads are lower than predicted. This may be explained by the strain-softening and the limited deformability of the concrete, which makes it highly unlikely that the uniaxial compressive strength be obtained at all points of the failure surface at the instant of

failure. Thus we are led to the introduction of an effective compressive strength f_c^* which is a fraction $\nu = f_c^*/f_c$ of the cylinder strength. (The effectiveness factor ν also occurs in other problems involving shear in concrete, cf. references [1],[2], and [3]). From Figure 15 it appears that ν is the smaller, the stronger the concrete.

In order to predict the ultimate load of a given punching problem, we need to assess the magnitude of the relative tensile strength ρ and the effectiveness factor ν. Accepting the argument that the presence of a support may disturb the failure surface formation, then from Figure 12 it appears that to get realistic results we should assume $\rho = 1/400$. This very low value suggests that the effectiveness factor on the tensile strength is much lower than on the compressive strength, as is to be expected considering the very reduced deformability of concrete in tension.

Having decided upon ρ we can find the effectiveness factor ν as the ratio between experimental and theoretical ultimate loads. This has been done for all the tests of Figures 14 and 15, except the two with the lowest support diameter (cf. Figure 15) for which no theoretical counterpart is defined. The result for the 54 tests is an average effectiveness factor of $\nu = 0.835$ with a coefficient of variation of 15.8%.

The aim of the experimental investigation carried out by KIERKEGAARD-HANSEN [10] was to develop a pull-out test to measure the compressive concrete strength. With imbedment depth and punch diameter constant at $d = h = 25$ mm, it was found that in order to ensure a good correlation between pull-out force and cylinder strength, the support diameter should not be greater than $D = 60$ mm, corresponding to $\tan\alpha_o = 0.70$, α_o being the half angle of the truncated cone punched out. This result agrees with the theory presented, since we found that the punching force would be influenced by the tensile strength if $\tan\alpha_o > \tan\varphi$. For concrete it is generally accepted that $\tan\varphi = 0.75$.

Based upon the experiments described in [10], the so-called lok-test apparatus was designed with D = 55 mm , corresponding to $\tan\alpha_o = 0.60$. Adhering strictly to the physical assumptions introduced, a failure surface with $\tan\alpha_o < \tan\varphi$ is not acceptable. However, as explained by JENSEN & BRÆSTRUP [7], this means that the pull-out force will be greater than predicted, but we would still expect a good correlation with the cylinder strength. That this is indeed the case is seen on Figure 16, which shows the results of lok-tests carried out at the Structural Research Laboratory [11]. The straight line is the theoretical relationship we would get by equation (9) if the angle of friction for concrete corresponded to $\tan\varphi=0.60$. As expected, the actual pull-out strengths are somewhat higher.

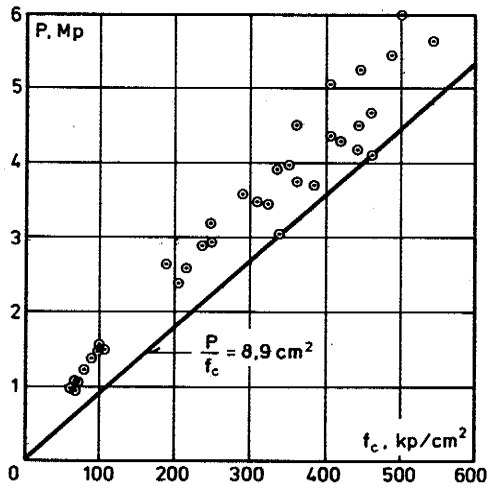

Figure 16: Pull-out force plotted against concrete cylinder strength. (test results from [11])

CONCLUSIONS

Based upon very simple physical assumptions (the modified Coulomb failure criterion with associated flow rule), the shape of the failure surface has been determined in good agreement with observations from punching and pull-out test. A ratio of $\rho = 1/400$ between tensile and compressive concrete strengths should be used in the formulae.

Then the ultimate load may be calculated, assuming an effective compressive concrete strength equal to 84% of the cylinder strength. The coefficient of variation is rather high (16%), indicating that the model does not give a quantitatively satisfactory description of the punching failure. It does, however, give a qualitative explanation of the phenomena observed. It further gives a theoretical foundation for the use of pull-out test to determine the compressive concrete strength, provided a suitable geometry of the test apparatus is specified.

ACKNOWLEDGEMENTS

The athours are currently studying the application of the theory of plasticity to punching shear with financial support from the Danish Council for Scientific and Technical Research. The research team is headed by professor M.P.Nielsen. The theoretical investigation described in the present report was carried out by civilingeniør M.W.Bræstrup during his research fellowship at the Structural Research Laboratory.

REFERENCES

[1] BRÆSTRUP, M.W.:
Plastic analysis of shear in reinforced concrete.
Magazine of Concrete Research Vol.26, No.89.
December 1974. pp.221-228

[2] NIELSEN, M.P. & BRÆSTRUP, M.W.:
Plastic shear strength of reinforced concrete beams.
Bygningsstatiske Meddelelser. Vol.46, No.3.
September 1975. pp.61-100.

[3] JENSEN, B.C.:
Lines of discontinuity for displacements in the theory of plasticity for plain and reinforced concrete.
Magazine of Concrete Research. Vol.27, No.92.
September 1975. pp.143-150.

[4] COURANT, R. & HILBERT, D.:
Methods of Mathematical Physics. Volume 1.
New York. Interscience Publishers, Inc. 1966. pp.561.

[5] KÆRN, J. & JENSEN, L.F.:
Gennemlokning af beton. (In Danish)
Copenhagen. Ren & Anvendt Mekanik, Danmarks Ingeniørakademi, Bygningsafdelingen. Report No.76:78. May 1976.
pp.34.

[6] Comité Européen du Béton:
Bulletin d'Information No.111. System of Unified Technical Regulations for Structures. Vol.II, Model Code for Structures in Concrete. October 1975.

[7] JENSEN, B.C. & BRÆSTRUP, M.W.:
Lok-tests determine the compressive strength of concrete.
Nordisk Betong. 1976 No.2. March 1976. pp.9-11.

[8] BACHE, H.H. & ISEN, J.C.:
Modal determination of concrete resistance to popout formation.
Journal of the ACI. Vol.65, No.6. June 1968. pp.445-450.

[9] HESS, U.:
Udtrækning af indstøbte inserts. (In Danish).
Copenhagen, Ren & Anvendt Mekanik, Danmarks Ingeniørakademi, Bygningsafdelingen. Report No.75:54.
January 1975. pp.25.

[10] KIERKEGAARD-HANSEN, P.:
Lok-strength.
Nordisk Betong. No.3. May 1975. pp.1-10.
(Test documentation supplied through a private communication).

[11] BRØNDUM-NIELSEN, T. & KRENCHEL, H.:
Lok-styrkeprøvning af beton. (In Danish).
Copenhagen, Structural Research Laboratory.
Technical University of Denmark. Sagsrapport Nr. S 3/69.
1974. pp.5.

SUMMARY

A slab on an annular support, centrally loaded by a circular punch, is considered. The concrete is assumed to be rigid, perfectly plastic, and as yield condition is used the modified Coulomb failure criterion with the associated flow rule (normality condition). The failure mechanism assumed consists in the punching out of a solid of revolution, the rest of the slab remaining rigid. Equating the rate of work done by the punch to the rate of work dissipated in the failure surface, an upper bound for the ultimate load is calculated.

The shape of the failure surface is determined by variational calculus. The generatrix is a catenary curve, possibly in combination with a straight line. The optimum diameter of the intersection with the bottom face of the slab and the corresponding ultimate load are found by iteration as functions of punch diameter, slab depth, and tensile and compressive concrete strengths.

With a certain support diameter, the failure surface degenerates into a truncated cone. In this case, the ultimate load is proportional to the compressive concrete strength, independently of the tensile strength.

The effects of shear reinforcement and of distributed counterpressure are studied.

The theoretical solution is compared with punching tests on slabs and pull-out tests on plain concrete specimens. Concerning the failure surface shape, the best agreement is obtained with the ratio of tensile to compressive concrete strength equal to 1/400. Using this value, the best agreement concerning the ultimate load is obtained with an effective compressive concrete strength equal to 84% of the cylinder strength, the coefficient of variation being 16%.

AFDELINGEN FOR BÆRENDE KONSTRUKTIONER
DANMARKS TEKNISKE HØJSKOLE

Structural Research Laboratory
Technical University of Denmark, DK-2800 Lyngby

RAPPORTER (Reports)

(1974 -)

R 43. BORCHERSEN,EGIL: Moiré pattern deformation theory and optical filtering techniques. 1974.
R 44. BRØNDUM-NIELSEN,TROELS: Optimum design of reinforced concrete shells and slabs. 1974.
R 45. PEDERSEN,FLEMMING BLIGAARD: Dynamic properties of anti-vibration mountings. 1974.
R 46. PHILIPSEN,CLAUS: Interferensholografisk bestemmelse af legemers form og flytningsfelt. 1974.
R 47. LARSEN,H.J. og H.RIBERHOLT: Tværbæreevne af søm og dykkere i spån- og træfiberplader. 1974.
R 48. POULSEN,P.E.: The photo-elastic effect in three--dimensional states of stress. 1974.
R 49. NIELSEN,J.: Modellove for kornede medier med særligt henblik på silomodeller. 1974.
R 50. KRENK,STEEN: The problems of an inclined crack in an elastic strip. 1974.
R 51. BRØNDUM-NIELSEN,TROELS: Effect of prestress on the damping of concrete. Effect of grouting on the fatique strength of post-tensioned concrete beams. 1974.
R 52. EGERUP,ARNE RYDÉN,H.J.LARSEN,H.RIBERHOLT and ERIK SØRENSEN: Papers presented at IUFRO-V, International Union of Forestry Research Organisation, Division V, Congress 1973. 1974.
R 53. HOLST,OLE: Automatic design of plane frames. 1974.
R 54. NIELSEN,SØREN: Svingninger i mastebarduner. 1974.
R 55. AGERSKOV,HENNING: Behaviour of connections using prestressed high strength bolts loaded in tension. 1974.
R 56. MØLLMANN,H.: Analysis of prestressed cable systems supported by elastic boundary structures. 1974.
R 57. NIELSEN,J. and V.ASKEGAARD: Scale errors in model tests on granular media with special reference to silo models. 1974.
R 58. SVENSSON,SVEN EILIF: Stability properties and mode interaction of continuous, conservative systems. 1974.
R 59. SIGBJÖRNSSON,RAGNAR: On the theory of structural vibrations due to natural wind. 1974.
R 60. SØRENSEN,HANS CHR.: Shear tests on 12 reinforced concrete T-beams. 1974.

R 61. NIELSEN,LEIF OTTO: Spændingshybride finite elementer til svingningsproblemer. 1975.
R 62. EGERUP,ARNE RYDÉN: Theoretical and experimental determination of the stiffness and ultimate load of timber trusses. 1975.
R 63. LAURSEN,MARTIN: A curved beam equilibrium element applicable in standard finite element program systems. 1975.
R 64. BACH,FINN: Metoder til måling af egenspændinger. 1975.
R 65. BACH,FINN: En teoretisk og eksperimentel undersøgelse af den akustoelastiske metodes anvendelighed til egenspændingsmåling. 1975.
R 66. PEDERSEN,FLEMMING BLIGAARD: Measurement of the complex modulus of viscoelastic materials. 1975.
R 67. PEDERSEN,FLEMMING BLIGAARD: Svingningsforsøg med viskoelastisk dæmpede sandwichbjælker. 1975.
R 68. AGERSKOV,HENNING: Analysis of high strength bolted connections subject to prying. A simplified approach. 1975.
R 69. PEDERSEN,MAX ELGAARD: En 2.ordens tilnærmelse til de konstitutive ligninger for beton. 1976.
R 70. RIBERHOLT,HILMER, and PETER CHR. NIELSEN: Timber under combined compression and bending stress. 1976.
R 71. KRENCHEL,HERBERT og J. BJØRNBAK-HANSEN: Undersøgelse af let konstruktionsbetons væsentligste materialeparametre. 1976.
R 72. BRÆSTRUP,M.W., M.P. NIELSEN, FINN BACH and B.CHR. JENSEN: Shear Tests on Reinforced Concrete T-Beams. Series T. 1976.
R 73. BRÆSTRUP,M.W., M.P. NIELSEN, FINN BACH and B.CHR. JENSEN: Plastic shear strength of reinforced concrete beams. 1976.
R 74. Resume-oversigt 1975. Summaries of papers 1975.